

# Chapter 2

## Problem Formulation

In this chapter, we describe the signal model, formulate the problem, and explain how differential beamforming works. We discuss the most fundamental performance measures such as the beampattern, the front-to-back ratio, the signal-to-noise ratio gain, the white noise gain, and the directivity factor. These measures are important in the evaluation of differential beamformers as well as in their derivation. We finally show how to obtain the most interesting theoretical beampatterns, of any order, associated with differential beamforming; they are the dipole, the cardioid, the hypercardioid, and the supercardioid.

### 2.1 Signal Model

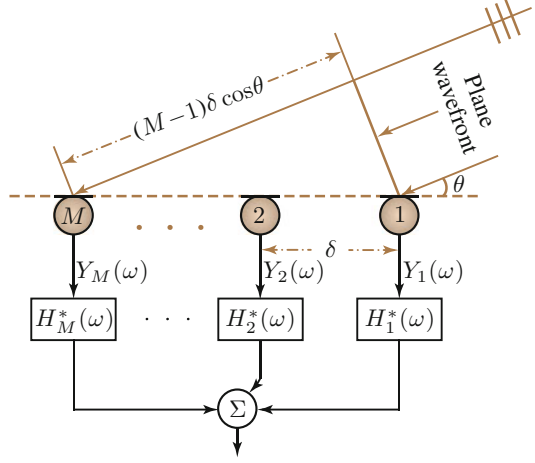
We consider a desired source signal (plane wave), in the farfield, that propagates from the azimuth angle,  $\theta$ , in an anechoic acoustic environment at the speed of sound, i.e.,  $c = 340$  m/s, and impinges on a uniform linear array consisting of  $M$  omnidirectional microphones (see Fig. 2.1). In this scenario, the corresponding steering vector (of length  $M$ ) is [1]

$$\mathbf{d}(\omega, \cos \theta) = \left[ 1 \ e^{-j\omega\delta \cos \theta/c} \ \dots \ e^{-j(M-1)\omega\delta \cos \theta/c} \right]^T, \quad (2.1)$$

where the superscript  $T$  is the transpose operator,  $j = \sqrt{-1}$  is the imaginary unit,  $\omega = 2\pi f$  is the angular frequency,  $f > 0$  is the temporal frequency, and  $\tau_0 = \delta/c$  is the delay between two successive sensors at the angle  $\theta = 0$ , with  $\delta$  being the interelement spacing. The acoustic wavelength is  $\lambda = c/f$ .

The focus of this work is on the design, with small apertures, of beamformers whose beampatterns are very close to the well-known theoretical DMA beampatterns; so only fixed directional beamformers are considered. For that, a complex weight,  $H_m^*(\omega)$ ,  $m = 1, 2, \dots, M$ , is applied at the output of each microphone, where the

**Fig. 2.1** A uniform linear microphone array with processing



superscript  $*$  denotes complex conjugation. The weighted outputs are then summed together to form the beamformer output as shown in Fig. 2.1. Putting all the gains together in a vector of length  $M$ , we get

$$\mathbf{h}(\omega) = [H_1(\omega) \ H_2(\omega) \ \cdots \ H_M(\omega)]^T. \quad (2.2)$$

Then, the objective is to design such a filter for any desired directivity pattern of any order.

Using the steering vector defined in (2.1), the observation signal vector of length  $M$  can be expressed in the frequency domain as [2]

$$\begin{aligned} \mathbf{y}(\omega) &= [Y_1(\omega) \ Y_2(\omega) \ \cdots \ Y_M(\omega)]^T \\ &= \mathbf{x}(\omega) + \mathbf{v}(\omega) \\ &= \mathbf{d}(\omega, \cos \theta) X(\omega) + \mathbf{v}(\omega), \end{aligned} \quad (2.3)$$

where  $Y_m(\omega)$  is the  $m$ th microphone signal,  $\mathbf{x}(\omega) = \mathbf{d}(\omega, \cos \theta) X(\omega)$ ,  $X(\omega)$  is the desired source signal, and  $\mathbf{v}(\omega)$  is the additive noise signal vector defined similarly to  $\mathbf{y}(\omega)$ .

To ensure that differential beamforming takes place, the following two assumptions are made [3–6].

- (i) The sensor spacing,  $\delta$ , is much smaller than the acoustic wavelength,  $\lambda = c/f$ , i.e.,  $\delta \ll \lambda$  (this implies that  $\omega\tau_0 \ll 2\pi$ ). This assumption is required so that the true acoustic pressure differentials can be approximated by finite differences of the microphones' outputs.
- (ii) The desired source signal propagates from the angle  $\theta = 0$  (endfire direction). Therefore, (2.3) becomes

$$\mathbf{y}(\omega) = \mathbf{d}(\omega, 1) X(\omega) + \mathbf{v}(\omega), \quad (2.4)$$

and, at the endfire, the value of the beamformer pattern should always be equal to 1 (or maximal).

Assumption (i) implies also that we can well approximate the exponential function that appears in the steering vector with the first few elements of its series expansion; so that frequency-invariant beamforming may be possible. Because of the symmetry of the steering vector, the only directions where we can design any desired beampatterns are at the endfires (0 and  $\pi$ ); in other directions, the beampattern design is very limited that is why Assumption (ii) is of great importance.

With the conventional linear approach, the beamformer output is simply [2]

$$\begin{aligned} Z(\omega) &= \sum_{m=1}^M H_m^*(\omega) Y_m(\omega) \\ &= \mathbf{h}^H(\omega) \mathbf{y}(\omega) \\ &= \mathbf{h}^H(\omega) \mathbf{d}(\omega, 1) X(\omega) + \mathbf{h}^H(\omega) \mathbf{v}(\omega), \end{aligned} \quad (2.5)$$

where  $Z(\omega)$  is the estimate of the desired signal,  $X(\omega)$ , and the superscript  $H$  is the conjugate-transpose operator. In our context, the distortionless constraint is desired, i.e.,

$$\mathbf{h}^H(\omega) \mathbf{d}(\omega, 1) = 1. \quad (2.6)$$

This means that the value of the beamformer pattern is equal to 1 at  $\theta = 0$  and smaller than 1 at  $\theta \neq 0$ .

## 2.2 Beampatterns

Each beamformer has a pattern of directional sensitivity, i.e., it has different sensitivities from sounds arriving from different directions. The beampattern or directivity pattern describes the sensitivity of the beamformer to a plane wave (source signal) impinging on the array from the direction  $\theta$ . Mathematically, it is defined as

$$\begin{aligned} \mathcal{B}[\mathbf{h}(\omega), \cos \theta] &= \mathbf{d}^H(\omega, \cos \theta) \mathbf{h}(\omega) \\ &= \sum_{m=1}^M H_m(\omega) e^{j(m-1)\omega\tau_0 \cos \theta}. \end{aligned} \quad (2.7)$$

The frequency-independent beampattern of a theoretical  $N$ th-order DMA is well known. It is defined as [4]

$$\begin{aligned}\mathcal{B}(\mathbf{a}_N, \cos \theta) &= \sum_{n=0}^N a_{N,n} \cos^n \theta \\ &= \mathbf{a}_N^T \mathbf{p}(\cos \theta),\end{aligned}\tag{2.8}$$

where  $a_{N,n}$ ,  $n = 0, 1, \dots, N$ , are real coefficients and

$$\begin{aligned}\mathbf{a}_N &= [a_{N,0} \ a_{N,1} \ \cdots \ a_{N,N}]^T, \\ \mathbf{p}(\cos \theta) &= [1 \ \cos \theta \ \cdots \ \cos^N \theta]^T.\end{aligned}$$

The different values of the coefficients  $a_{N,n}$ ,  $n = 0, 1, \dots, N$  determine the different directivity patterns of the  $N$ th-order DMA. It may be convenient to use a normalization convention for the coefficients. For that, in the direction of the desired signal, i.e., for  $\theta = 0$ , we would like the beampattern to be equal to 1, i.e.,  $\mathcal{B}(\mathbf{a}_N, 1) = 1$ . Therefore, we have

$$\sum_{n=0}^N a_{N,n} = 1.\tag{2.9}$$

As a result, we may choose the first coefficient as

$$a_{N,0} = 1 - \sum_{n=1}^N a_{N,n}.\tag{2.10}$$

All interesting beampatterns have at least one null in some direction. Since  $\cos \theta$  is an even function, so is  $\mathcal{B}(\mathbf{a}_N, \cos \theta)$ . Therefore, on a polar plot,<sup>1</sup>  $\mathcal{B}(\mathbf{a}_N, \cos \theta)$  is symmetric about the axis  $0 - \pi$  and any DMA beampattern design can be restricted to this range. It follows from (2.8) that an  $N$ th-order directivity pattern has at most  $N$  (distinct) nulls in this range.

## 2.3 Front-to-Back Ratios

The front-to-back ratio (FBR) is defined as the ratio of the power of the output of the array to signals propagating from the front-half plane to the output power for signals arriving from the rear-half plane [7]. This ratio, for the spherically isotropic (diffuse) noise field, is mathematically defined as [7]

---

<sup>1</sup>Polar patterns are a very convenient way to describe the directional sensitivity of the DMAs.

$$\begin{aligned}
\mathcal{F}[\mathbf{h}(\omega)] &= \frac{\int_0^{\pi/2} |\mathcal{B}[\mathbf{h}(\omega), \cos \theta]|^2 \sin \theta d\theta}{\int_{\pi/2}^{\pi} |\mathcal{B}[\mathbf{h}(\omega), \cos \theta]|^2 \sin \theta d\theta} \\
&= \frac{\mathbf{h}^H(\omega) \mathbf{\Gamma}_{0,\pi/2}(\omega) \mathbf{h}(\omega)}{\mathbf{h}^H(\omega) \mathbf{\Gamma}_{\pi/2,\pi}(\omega) \mathbf{h}(\omega)},
\end{aligned} \tag{2.11}$$

where

$$\mathbf{\Gamma}_{0,\pi/2}(\omega) = \int_0^{\pi/2} \mathbf{d}(\omega, \cos \theta) \mathbf{d}^H(\omega, \cos \theta) \sin \theta d\theta, \tag{2.12}$$

$$\mathbf{\Gamma}_{\pi/2,\pi}(\omega) = \int_{\pi/2}^{\pi} \mathbf{d}(\omega, \cos \theta) \mathbf{d}^H(\omega, \cos \theta) \sin \theta d\theta. \tag{2.13}$$

Now, let us compute the entries of the matrix:

$$\mathbf{\Gamma}_{\psi_1, \psi_2}(\omega) = \mathcal{N}_{\psi_1, \psi_2} \int_{\psi_1}^{\psi_2} \mathbf{d}(\omega, \cos \theta) \mathbf{d}^H(\omega, \cos \theta) \sin \theta d\theta, \tag{2.14}$$

where

$$\begin{aligned}
\mathcal{N}_{\psi_1, \psi_2} &= \frac{1}{\int_{\psi_1}^{\psi_2} \sin \theta d\theta} \\
&= \frac{1}{\cos \psi_1 - \cos \psi_2}
\end{aligned} \tag{2.15}$$

is a normalization term. The  $(i, j)$ th element (with  $i, j = 1, 2, \dots, M$ ) of  $\mathbf{\Gamma}_{\psi_1, \psi_2}(\omega)$  can be written as

$$\begin{aligned}
[\mathbf{\Gamma}_{\psi_1, \psi_2}(\omega)]_{ij} &= \mathcal{N}_{\psi_1, \psi_2} \int_{\psi_1}^{\psi_2} e^{-j\omega(i-1)\tau_0 \cos \theta} e^{j\omega(j-1)\tau_0 \cos \theta} \sin \theta d\theta \\
&= \mathcal{N}_{\psi_1, \psi_2} \int_{\psi_1}^{\psi_2} e^{j\omega(j-i)\tau_0 \cos \theta} \sin \theta d\theta \\
&= -\mathcal{N}_{\psi_1, \psi_2} \int_{\cos \psi_1}^{\cos \psi_2} e^{j\omega(j-i)\tau_0 u} du \\
&= \mathcal{N}_{\psi_1, \psi_2} \int_{\cos \psi_2}^{\cos \psi_1} e^{j\omega(j-i)\tau_0 u} du.
\end{aligned} \tag{2.16}$$

Therefore, we deduce that

$$[\mathbf{\Gamma}_{\psi_1, \psi_2}(\omega)]_{ij} = \mathcal{N}_{\psi_1, \psi_2} \frac{e^{J\omega(j-i)\tau_0 \cos \psi_1} - e^{J\omega(j-i)\tau_0 \cos \psi_2}}{J\omega(j-i)\tau_0}, \quad (2.17)$$

with

$$[\mathbf{\Gamma}_{\psi_1, \psi_2}(\omega)]_{mm} = 1, \quad m = 1, 2, \dots, M. \quad (2.18)$$

As a result, the elements of the  $M \times M$  matrices  $\mathbf{\Gamma}_{0, \pi/2}(\omega)$  and  $\mathbf{\Gamma}_{\pi/2, \pi}(\omega)$  are, respectively,

$$[\mathbf{\Gamma}_{0, \pi/2}(\omega)]_{ij} = \frac{e^{J\omega(j-i)\tau_0} - 1}{J\omega(j-i)\tau_0} \quad (2.19)$$

and

$$[\mathbf{\Gamma}_{\pi/2, \pi}(\omega)]_{ij} = \frac{1 - e^{-J\omega(j-i)\tau_0}}{J\omega(j-i)\tau_0}, \quad (2.20)$$

with  $[\mathbf{\Gamma}_{0, \pi/2}(\omega)]_{mm} = [\mathbf{\Gamma}_{\pi/2, \pi}(\omega)]_{mm} = 1, \quad m = 1, 2, \dots, M.$

For the spherically isotropic noise field, the frequency-independent FBR of a theoretical  $N$ th-order DMA is defined as [4]

$$\mathcal{F}(\mathbf{a}_N) = \frac{\int_0^{\pi/2} \mathcal{B}^2(\mathbf{a}_N, \cos \theta) \sin \theta d\theta}{\int_{\pi/2}^{\pi} \mathcal{B}^2(\mathbf{a}_N, \cos \theta) \sin \theta d\theta}. \quad (2.21)$$

## 2.4 Signal-to-Noise Ratio Gains

If we take microphone 1 as the reference, we can define the input signal-to-noise ratio (SNR) with respect to this reference as

$$\text{iSNR}(\omega) = \frac{\phi_X(\omega)}{\phi_{V_1}(\omega)}, \quad (2.22)$$

where  $\phi_X(\omega) = E[|X(\omega)|^2]$  and  $\phi_{V_1}(\omega) = E[|V_1(\omega)|^2]$  are the variances of  $X(\omega)$  and  $V_1(\omega)$ , respectively, with  $E[\cdot]$  denoting mathematical expectation.

The output SNR is defined as

$$\begin{aligned} \text{oSNR}[\mathbf{h}(\omega)] &= \phi_X(\omega) \frac{|\mathbf{h}^H(\omega) \mathbf{d}(\omega, 1)|^2}{\mathbf{h}^H(\omega) \mathbf{\Phi}_v(\omega) \mathbf{h}(\omega)} \\ &= \frac{\phi_X(\omega)}{\phi_{V_1}(\omega)} \times \frac{|\mathbf{h}^H(\omega) \mathbf{d}(\omega, 1)|^2}{\mathbf{h}^H(\omega) \mathbf{\Gamma}_v(\omega) \mathbf{h}(\omega)}, \end{aligned} \quad (2.23)$$

where

$$\mathbf{\Phi}_v(\omega) = E[\mathbf{v}(\omega) \mathbf{v}^H(\omega)] \quad (2.24)$$

and

$$\mathbf{\Gamma}_v(\omega) = \frac{\mathbf{\Phi}_v(\omega)}{\phi_{V_1}(\omega)} \quad (2.25)$$

are the correlation and pseudo-coherence matrices of  $\mathbf{v}(\omega)$ , respectively.

The definition of the SNR gain is easily derived from the two previous definitions of the input and output SNRs, i.e.,

$$\begin{aligned} \mathcal{G}[\mathbf{h}(\omega)] &= \frac{\text{oSNR}[\mathbf{h}(\omega)]}{\text{iSNR}(\omega)} \\ &= \frac{|\mathbf{h}^H(\omega) \mathbf{d}(\omega, 1)|^2}{\mathbf{h}^H(\omega) \mathbf{\Gamma}_v(\omega) \mathbf{h}(\omega)}. \end{aligned} \quad (2.26)$$

Assume that the matrix  $\mathbf{\Gamma}_v(\omega)$  is nonsingular. In this case, for any two vectors  $\mathbf{h}(\omega)$  and  $\mathbf{d}(\omega, 1)$ , we have

$$|\mathbf{h}^H(\omega) \mathbf{d}(\omega, 1)|^2 \leq [\mathbf{h}^H(\omega) \mathbf{\Gamma}_v(\omega) \mathbf{h}(\omega)] [\mathbf{d}^H(\omega, 1) \mathbf{\Gamma}_v^{-1}(\omega) \mathbf{d}(\omega, 1)], \quad (2.27)$$

with equality if and only if  $\mathbf{h}(\omega) \propto \mathbf{\Gamma}_v^{-1}(\omega) \mathbf{d}(\omega, 1)$ . Using the inequality (2.27) in (2.26), we deduce an upper bound for the gain:

$$\begin{aligned} \mathcal{G}[\mathbf{h}(\omega)] &\leq \mathbf{d}^H(\omega, 1) \mathbf{\Gamma}_v^{-1}(\omega) \mathbf{d}(\omega, 1) \\ &\leq \text{tr}[\mathbf{\Gamma}_v^{-1}(\omega)] \text{tr}[\mathbf{d}(\omega, 1) \mathbf{d}^H(\omega, 1)] \\ &\leq M \text{tr}[\mathbf{\Gamma}_v^{-1}(\omega)], \end{aligned} \quad (2.28)$$

where  $\text{tr}[\cdot]$  is the trace of a square matrix. We observe how the gain is upper bounded [as long as  $\mathbf{\Gamma}_v(\omega)$  is nonsingular] and depends on the number of microphones as well as on the nature of the noise.

The most convenient way to evaluate the sensitivity of the array to some of its imperfections is via the so-called white noise gain (WNG), which is defined by taking  $\mathbf{\Gamma}_v(\omega) = \mathbf{I}_M$  in (2.26), where  $\mathbf{I}_M$  is the  $M \times M$  identity matrix, i.e.,

$$\mathcal{W}[\mathbf{h}(\omega)] = \frac{|\mathbf{h}^H(\omega) \mathbf{d}(\omega, 1)|^2}{\mathbf{h}^H(\omega) \mathbf{h}(\omega)}. \quad (2.29)$$

The WNG is, obviously, the SNR gain in the presence of spatially white noise. Using the Cauchy-Schwarz inequality, i.e.,

$$|\mathbf{h}^H(\omega) \mathbf{d}(\omega, 1)|^2 \leq [\mathbf{h}^H(\omega) \mathbf{h}(\omega)] [\mathbf{d}^H(\omega, 1) \mathbf{d}(\omega, 1)], \quad (2.30)$$

we easily deduce from (2.29) that

$$\mathcal{W}[\mathbf{h}(\omega)] \leq M, \quad \forall \mathbf{h}(\omega). \quad (2.31)$$

As a result, the maximum WNG is

$$\mathcal{W}_{\max} = M, \quad (2.32)$$

which is frequency independent. The white noise amplification is the most serious problem in differential beamforming.

Another important measure, which quantifies how the microphone array performs in the presence of reverberation is the directivity factor (DF). Considering the spherically isotropic noise field, the DF is defined as

$$\begin{aligned} \mathcal{D}[\mathbf{h}(\omega)] &= \frac{|\mathcal{B}[\mathbf{h}(\omega), 1]|^2}{\frac{1}{2} \int_0^\pi |\mathcal{B}[\mathbf{h}(\omega), \cos \theta]|^2 \sin \theta d\theta} \\ &= \frac{|\mathbf{h}^H(\omega) \mathbf{d}(\omega, 1)|^2}{\mathbf{h}^H(\omega) \mathbf{\Gamma}_{0,\pi}(\omega) \mathbf{h}(\omega)}, \end{aligned} \quad (2.33)$$

where

$$\mathbf{\Gamma}_{0,\pi}(\omega) = \frac{1}{2} \int_0^\pi \mathbf{d}(\omega, \cos \theta) \mathbf{d}^H(\omega, \cos \theta) \sin \theta d\theta. \quad (2.34)$$

From (2.17) and (2.18), we find that the elements of the  $M \times M$  matrix  $\mathbf{\Gamma}_{0,\pi}(\omega)$  are

$$\begin{aligned} [\mathbf{\Gamma}_{0,\pi}(\omega)]_{ij} &= \frac{\sin[\omega(j-i)\tau_0]}{\omega(j-i)\tau_0} \\ &= \text{sinc}[\omega(j-i)\tau_0], \end{aligned} \quad (2.35)$$

with  $[\mathbf{\Gamma}_{0,\pi}(\omega)]_{mm} = 1$ ,  $m = 1, 2, \dots, M$ . The DF is, obviously, the SNR gain in the presence of diffuse noise. Again, by invoking the Cauchy-Schwarz inequality, i.e.,

$$|\mathbf{h}^H(\omega) \mathbf{d}(\omega, 1)|^2 \leq [\mathbf{h}^H(\omega) \mathbf{\Gamma}_{0,\pi}(\omega) \mathbf{h}(\omega)] [\mathbf{d}^H(\omega, 1) \mathbf{\Gamma}_{0,\pi}^{-1}(\omega) \mathbf{d}(\omega, 1)], \quad (2.36)$$

we find from (2.33) that

$$\mathcal{D}[\mathbf{h}(\omega)] \leq \mathbf{d}^H(\omega, 1) \mathbf{\Gamma}_{0,\pi}^{-1}(\omega) \mathbf{d}(\omega, 1), \quad \forall \mathbf{h}(\omega). \quad (2.37)$$

As a result, the maximum DF is

$$\mathcal{D}_{\max}(\omega) = \mathbf{d}^H(\omega, 1) \mathbf{\Gamma}_{0,\pi}^{-1}(\omega) \mathbf{d}(\omega, 1), \quad (2.38)$$

which is frequency dependent, and it can be shown that [8]

$$\lim_{\delta \rightarrow 0} \mathcal{D}_{\max}(\omega) = M^2. \quad (2.39)$$

For the spherically isotropic noise field, the frequency-independent DF of a theoretical  $N$ th-order DMA is defined as [4]

$$\mathcal{D}(\mathbf{a}_N) = \frac{\mathcal{B}^2(\mathbf{a}_N, 1)}{\frac{1}{2} \int_0^\pi \mathcal{B}^2(\mathbf{a}_N, \cos \theta) \sin \theta d\theta}. \quad (2.40)$$

## 2.5 Examples of Theoretical Differential Beamformers

The most well-known and studied  $N$ th-order DMA beampatterns are the dipole, the cardioid, the hypercardioid, and the supercardioid.

The  $N$ th-order dipole has a unique null with multiplicity  $N$  in the direction  $\pi/2$ . Its beampattern is then given by

$$\mathcal{B}_{N,\text{Dp}}(\cos \theta) = \cos^N \theta, \quad (2.41)$$

implying that  $a_{N,N} = 1$  and  $a_{N,N-1} = a_{N,N-2} = \dots = a_{N,0} = 0$ .

The  $N$ th-order cardioid has a unique null with multiplicity  $N$  in the direction  $\pi$ . Its beampattern is then given by

$$\begin{aligned} \mathcal{B}_{N,\text{Cd}}(\cos \theta) &= \frac{1}{2^N} (1 + \cos \theta)^N \\ &= \sum_{n=0}^N \frac{N!}{2^N n!(N-n)!} \cos^n \theta, \end{aligned} \quad (2.42)$$

implying that

$$a_{N,n} = \frac{N!}{2^N n!(N-n)!}, \quad n = 0, 1, \dots, N. \quad (2.43)$$

The coefficients of the  $N$ th-order hypercardioid can be obtained by maximizing the DF,  $\mathcal{D}(\mathbf{a}_N)$ , given in (2.40). It can be shown that [4]

$$\mathcal{D}(\mathbf{a}_N) = \frac{\mathbf{a}_N^T \mathbf{1} \mathbf{1}^T \mathbf{a}_N}{\mathbf{a}_N^T \mathbf{H}_N \mathbf{a}_N}, \quad (2.44)$$

where

$$\mathbf{1} = [1 \ 1 \ \dots \ 1]^T$$

is a vector of length  $N + 1$  and  $\mathbf{H}_N$  is a Hankel matrix [of size  $(N + 1) \times (N + 1)$ ] whose elements are given by

$$[\mathbf{H}_N]_{ij} = \begin{cases} \frac{1}{1 + i + j}, & \text{if } i + j \text{ even} \\ 0, & \text{otherwise} \end{cases}, \quad (2.45)$$

with  $i, j = 0, 1, \dots, N$ . In (2.44), we recognize the generalized Rayleigh quotient. Therefore, the vector  $\mathbf{a}_N$  that maximizes  $\mathcal{D}(\mathbf{a}_N)$  is the eigenvector corresponding to the maximum eigenvalue of the matrix  $\mathbf{H}_N^{-1} \mathbf{1} \mathbf{1}^T$ , i.e.,

$$\mathbf{a}_{N,\max} = \frac{\mathbf{H}_N^{-1} \mathbf{1}}{\mathbf{1}^T \mathbf{H}_N^{-1} \mathbf{1}}. \quad (2.46)$$

As a result, the beampattern of the  $N$ th-order hypercardioid is

$$\mathcal{B}_{N,\text{Hd}}(\cos \theta) = \frac{\mathbf{1}^T \mathbf{H}_N^{-1} \mathbf{p}(\cos \theta)}{\mathbf{1}^T \mathbf{H}_N^{-1} \mathbf{1}}. \quad (2.47)$$

The coefficients of the  $N$ th-order supercardioid can be obtained by maximizing the FBR,  $\mathcal{F}(\mathbf{a}_N)$ , defined in (2.21). It can be shown that [4]

$$\mathcal{F}(\mathbf{a}_N) = \frac{\mathbf{a}_N^T \mathbf{H}_N'' \mathbf{a}_N}{\mathbf{a}_N^T \mathbf{H}_N' \mathbf{a}_N}, \quad (2.48)$$

where  $\mathbf{H}_N'$  and  $\mathbf{H}_N''$  are two Hankel matrices [of size  $(N + 1) \times (N + 1)$ ] whose elements are given by, respectively,

$$[\mathbf{H}_N']_{ij} = \frac{(-1)^{i+j}}{1 + i + j} \quad (2.49)$$

and

$$[\mathbf{H}_N'']_{ij} = \frac{1}{1 + i + j}, \quad (2.50)$$

with  $i, j = 0, 1, \dots, N$ . Let us denote by  $\mathbf{a}'_{N,\max}$  the eigenvector corresponding to the maximum eigenvalue of  $\mathbf{H}_N'^{-1} \mathbf{H}_N''$ . Then,  $\mathbf{a}'_{N,\max}$  maximizes the FBR and the beampattern of the  $N$ th-order supercardioid is

$$\mathcal{B}_{N,\text{Sd}}(\cos \theta) = \frac{\mathbf{a}'_{N,\max}{}^T \mathbf{p}(\cos \theta)}{\mathbf{a}'_{N,\max}{}^T \mathbf{p}(1)}. \quad (2.51)$$

The most well-known first-order directivity patterns are expressed as

$$\mathcal{B}_{1,\text{Dp}}(\cos \theta) = \cos \theta, \quad (2.52)$$

$$\mathcal{B}_{1,\text{Cd}}(\cos \theta) = \frac{1}{2} + \frac{1}{2} \cos \theta, \quad (2.53)$$

$$\mathcal{B}_{1,\text{Hd}}(\cos \theta) = \frac{1}{4} + \frac{3}{4} \cos \theta, \quad (2.54)$$

$$\mathcal{B}_{1,\text{Sd}}(\cos \theta) = \frac{\sqrt{3}-1}{2} + \frac{3-\sqrt{3}}{2} \cos \theta. \quad (2.55)$$

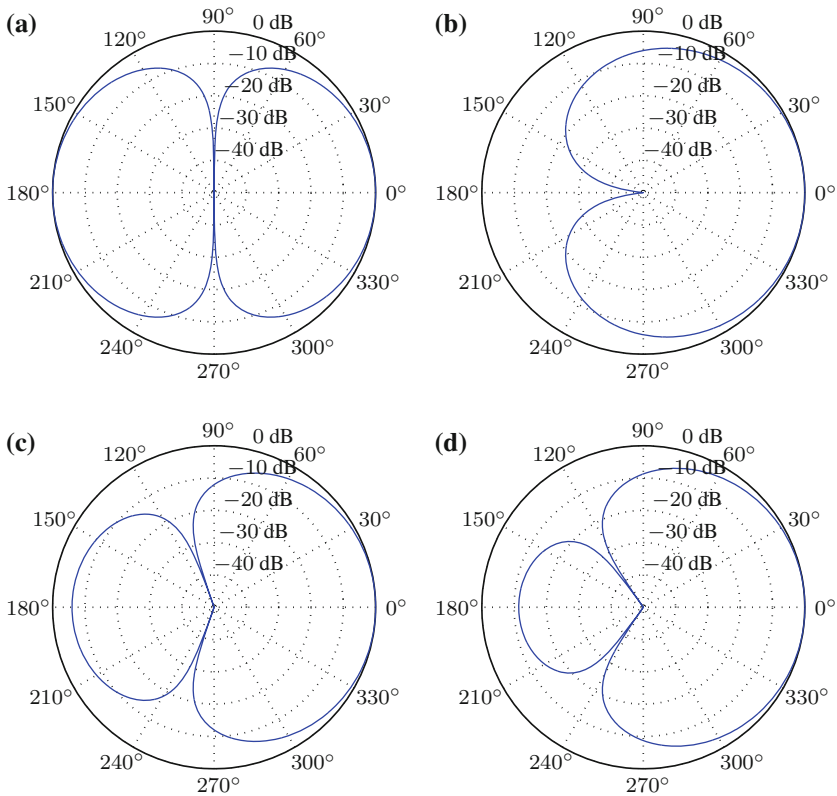


**Fig. 2.2** First-order directivity patterns: **a** dipole, **b** cardioid, **c** hypercardioid, and **d** supercardioid

Figure 2.2 shows these different polar patterns. What is exactly shown are the values of the magnitude squared beampattern in dB, i.e.,  $10 \log_{10} \mathcal{B}^2(\mathbf{a}_N, \cos \theta)$ .

The most interesting second-order directivity patterns are given by

$$\mathcal{B}_{2,\text{Dp}}(\cos \theta) = \cos^2 \theta, \quad (2.56)$$

$$\mathcal{B}_{2,\text{Cd}}(\cos \theta) = \frac{1}{4} + \frac{1}{2} \cos \theta + \frac{1}{4} \cos^2 \theta, \quad (2.57)$$

$$\mathcal{B}_{2,\text{Hd}}(\cos \theta) = -\frac{1}{6} + \frac{1}{3} \cos \theta + \frac{5}{6} \cos^2 \theta, \quad (2.58)$$

$$\mathcal{B}_{2,\text{Sd}}(\cos \theta) = \frac{1}{2(3 + \sqrt{7})} + \frac{\sqrt{7}}{3 + \sqrt{7}} \cos \theta + \frac{5}{2(3 + \sqrt{7})} \cos^2 \theta. \quad (2.59)$$

Figure 2.3 depicts the different second-order directivity patterns given above.

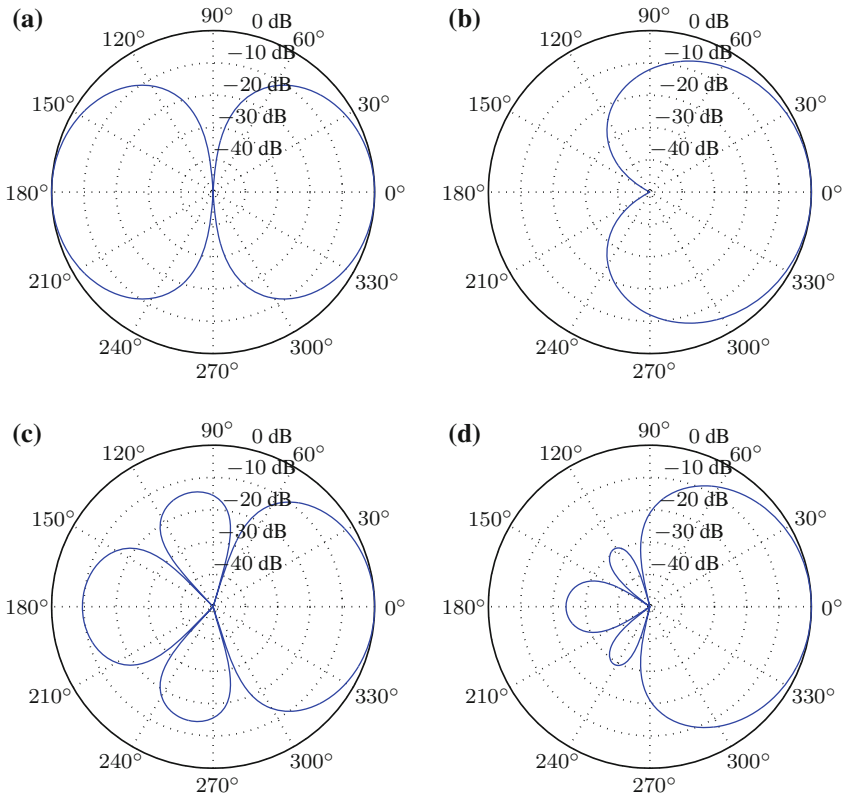


**Fig. 2.3** Second-order directivity patterns: **a** dipole, **b** cardioid, **c** hypercardioid, and **d** supercardioid

The most important third-order directivity patterns are expressed as

$$\mathcal{B}_{3,\text{Dp}}(\cos \theta) = \cos^3 \theta, \quad (2.60)$$

$$\mathcal{B}_{3,\text{Cd}}(\cos \theta) = \frac{1}{8} + \frac{3}{8} \cos \theta + \frac{3}{8} \cos^2 \theta + \frac{1}{8} \cos^3 \theta, \quad (2.61)$$

$$\mathcal{B}_{3,\text{Hd}}(\cos \theta) = -\frac{3}{32} - \frac{15}{32} \cos \theta + \frac{15}{32} \cos^2 \theta + \frac{35}{32} \cos^3 \theta, \quad (2.62)$$

$$\mathcal{B}_{3,\text{Sd}}(\cos \theta) \approx 0.0184 + 0.2004 \cos \theta + 0.4750 \cos^2 \theta + 0.3061 \cos^3 \theta. \quad (2.63)$$

Figure 2.4 depicts the different third-order directivity patterns given above.

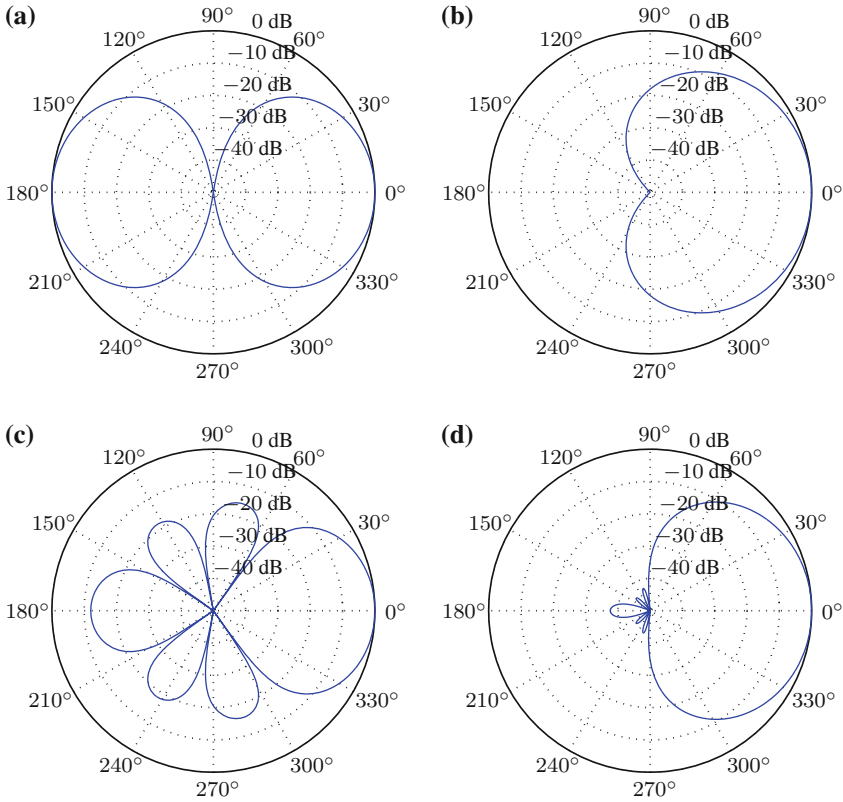


**Fig. 2.4** Third-order directivity patterns: **a** dipole, **b** cardioid, **c** hypercardioid, and **d** supercardioid

## References

1. Johnson DH, Dudgeon DE (1993) Array signal processing: concepts and techniques. Signal processing series. Englewood Cliffs, Prentice-Hall
2. Benesty J, Chen J, Huang Y (2008) Microphone array signal processing. Springer, Berlin
3. Elko GW, Meyer J (2008) Microphone arrays. In: Benesty J, Sondhi MM, Huang Y (eds) Springer handbook of speech processing. Springer, Berlin, Chapter 50, pp 1021–1041
4. Elko GW (2000) Superdirectional microphone arrays In: Gay SL, Benesty J (eds) Acoustic signal processing for telecommunication. Kluwer Academic Publishers, Boston, MA, Chapter 10, pp 181–237
5. Benesty J, Chen J (2012) Study and design of differential microphone arrays. Springer, Berlin
6. Chen J, Benesty J, Pan C (2014) On the design and implementation of linear differential microphone arrays. *J Acoust Soc Am* 136:3097–3113
7. Marshall RN, Harry WR (1941) A new microphone providing uniform directivity over an extended frequency range. *J Acoust Soc Am* 12:481–497
8. Uzkov AI (1946) An approach to the problem of optimum directive antenna design. *Comptes Rendus (Doklady) de l'Academie des Sciences de l'URSS*, vol LIII no 1, pp 35–38

Fundamentals of Differential Beamforming

Benesty, J.; Chen, J.; Pan, C.

2016, VIII, 122 p. 79 illus., 77 illus. in color., Softcover

ISBN: 978-981-10-1045-3